and this interaction correlates with transformation (*4*). Point mutants of Bcr-Abl that are defective in transformation still bound Grb-2, indicating that they can activate Ras (*4*, *5*). This activity demonstrates that, whereas Grb-2 binding is necessary for transformation, it is not sufficient. Transformation by the Grb-2 binding mutant was not enhanced by the overexpression of Myc, suggesting that Myc and Ras may operate in different pathways.

REFERENCES AND NOTES

1. B. Vogelstein and K. W. Kinzler, *Trends Genet.* **9**, 138 (1993).
2. Shtivelman, B. Lifshitz, R. P. Gale, E. Canaani, *Nature* **315**, 550 (1985); S. C. Clark *et al.*, *Science* **239**, 775 (1988).
3. A. M. Pendergast, M. L. Gishizky, M. H. Havlik, O. N. Witte, *Mol. Cell. Biol.* **13**, 1728 (1993).
4. A. M. Pendergast *et al.*, *Cell* **75**, 175 (1993).
5. E. J. Lowenstein *et al.*, *ibid.* **70**, 431 (1992); K. Baltensperger *et al.*, *Science* **260**, 1950 91993); L. Buday and J. Downward, *Cell* **73**, 611 (1993); S. E. Egan *et al.*, *Nature* **363**, 45 (1993); N. W. Gale, S. Kaplan, E. J. Lowenstein, J. Schlessinger, D. Bar-Sagi, *ibid.*, p. 88; N. Li *et al.*, *ibid.*, p. 85; J. P. Olivier *et al.*, *Cell* **73**, 179 (1993); M. Rozakis-Adcock, R. Fernley, J. Wade, T. Pawson, D. Bowtell, *Nature* **363**, 83 (1993); A. Simon, G. S. Dodson, G. M. Rubin, *Cell* **73**, 169 (1993); E. Y. Skolnik *et al.*, *Science* **260**, 1953 (1993).
6. C. A. Koch, D. Anderson, M. F. Moran, C. Ellis, T. Pawson, *Science* **252**, 668 (1991). Abbreviations for the amino acid residues are as follows: A, Ala; C, Cys; D, Asp; E, Glu; F, Phe; G, Gly; H, His; I, Ile; K, Lys; L, Leu; M, Met; N, Asn; P, Pro; Q, Gln; R, Arg; S, Ser; T, Thr; V, Val; W, Trp; and Y, Tyr.
7. G. Waksman *et al.*, *Nature* **358**, 646 (1992).
8. M. F. Verderame, J. M. Kaplan, H. E. Varmus, *J. Virol.* **63**, 338 (1989); H. Hirai and H. E. Varmus, *Genes Dev.* **4**, 2342 (1990); B. J. Mayer, P. K. Jackson, R. A. Van Etten, D. Baltimore, *Mol. Cell. Biol.* **12**, 609 (1992).
9. The mutation in the FLVRES motif of P185 Bcr-Abl was generated by polymerase chain reaction (PCR)–based mutagenesis. The mutagenic oligonucleotide 5′ primer used to replace Arg^{552} in the SH2 domain of P185 with Leu was 5′-TATCCGCTGAGCAGCGGGATCAATGGCAGCTTCTTGGTGCTTGAGAGTGAGAGCAGTCC-3′, where the underlined sequence replaced the WT codon of CGT. The downstream primer used was 3′-CGTAAACCTCATAACGAAACCTTCGAACGC-5′. Sequences of *c-abl* were used as a template to PCR-amplify the mutant SH2 domain. The PCR product was subcloned into *c-abl* pBluescript (Stratagene) and analyzed by dideoxy DNA sequencing (Sequenase, United States Biochemical) to verify the presence of the point mutation. The FLVRES mutation was then reconstructed into Bcr-Abl by ligation of a Kpn I and Hind III digest of *c-abl* FLVRES mutant to an Eco RI and Kpn I digest of P185 *bcr-abl*. The P185 FLVRES mutant was then subcloned into the pSRαMSVtkneo retroviral vector (*10*) as an Eco RI and Hind III fragment. The autophosphorylation mutant P185 Y813F was generated by the recombination of the 5′ end of P185 *bcr-abl* with a Kpn I and Hind III fragment of P210 *bcr-abl* 1294F (*3*). To generate the double mutant P185 L552 and F813, P185 Y813F was digested with Bsr GI and Hind III and recombined with the 5′ end of P185 R552L.
10. A. J. Muller *et al.*, *Mol. Cell. Biol.* **11**, 1785 (1991).
11. Possible identities of p62 and p65 include previously identified molecules such as the Ras–guanosine triphosphatase activating protein–associated p62, the protein tyrosine phosphatase Syp, and the p66 isoform of Shc. G. Wong *et al.*, *Cell* **69**, 551 (1992); G.-S. Feng, C.-C. Hui, T. Pawson, *Science* **259**, 1607 (1993); J. McGlade, A. Cheng, G. Pelicci, P. G. Pelicci, T. Pawson, *Proc. Natl. Acad. Sci. U.S.A.* **89**, 8869 (1992).
12. A fraction of Grb-2 molecules was found to undergo a mobility shift within cells expressing all P185 forms, excluding cells expressing P185 Y177F. Immunoblot analysis with antibody to phosphotyrosine revealed that the upper band was tyrosine-phosphorylated Grb-2, which may be the result of Bcr-Abl overexpression in 293T cells.
13. T. Lugo and O. N. Witte, *Mol. Cell. Biol.* **9**, 1263 (1989).
14. C. L. Sawyers, W. Callahan, O. N. Witte, *Cell* **70**, 901 (1992).
15. Three independent transformed colonies were isolated and expanded in tissue culture. Bcr-Abl expression, intracellular phosphotyrosine concentrations, and DNA sequencing confirmed the presence of the FLVRES mutation. Protein immunoblot analysis of transformed colonies with antibody to phosphotyrosine gave results indistinguishable from those shown in Fig. 1.
16. M. F. Roussel, J. L. Cleveland, S. A. Shurtleff, C. J. Sherr, *Nature* **353**, 361 (1991).
17. J. E. DeClue, K. Zhang, P. Redford, W. C. Vass, D. R. Lowy, *Mol. Cell. Biol.* **11**, 2819 (1991); S. M. Thomas, M. DeMarco, G. D'Arcangelo, S. Halegoua, J. S. Brugge, *Cell* **68**, 1031 (1992); K. W. Wood, C. Sarnecki, T. M. Roberts, J. Blenis, *ibid.*, p. 1041.
18. C. L. Sawyers, J. McLaughlin, M. Havlik, O. N. Witte, in preparation.
19. L. Puil *et al.*, *EMBO J.*, in press.
20. R. B. DuBridge *et al.*, *Mol. Cell. Biol.* **7**, 379 (1987).
21. J. B. Konopka and O. N. Witte, *ibid.* **5**, 3116 (1985).
22. Soft agar transformation by Bcr-Abl forms was determined as described in (*10*, *13*). Infected cells were grown for 2 days in culture before selection in G418 for 14 days. Cell populations were then superinfected with *neo* retrovirus or human *c-myc* retrovirus (*14*). 48 hours after infection, cells were plated in agar at a density of 5×10^4 cells per 6-cm dish. The samples were plated in duplicate in medium containing fetal calf serum (20%). Colonies equal to and larger than 0.5 mm in size were counted for 2 to 3 weeks after growth in soft agar. The numbers of colonies grown in soft agar represent averages from five independent experiments for cells expressing WT P185. Colonies expressing mutant P185 proteins were averaged from two to three independent experiments. Large colonies (L) represent sizes ranging from 0.5 to 3.0 mm in diameter. Small colonies (S) represent visually detectable colonies ≤0.5 mm in diameter. G418-resistant populations expressing P185 proteins were superinfected with retrovirus containing the *neo* gene or retrovirus containing *c-myc*.

23. We thank A. M. Pendergast for providing the Grb-2 binding mutant of Bcr-Abl (P185 Y177F); S. Smale, D. Black, A. Berk, L. Zipursky, D. Saffran, and L. Cohen for critical review of the manuscript; S. Quan and J. C. White for photography; and J. Shimaoka for assistance in preparation of the manuscript. D.E.H.A. is a fellow of the Medical Research Council of Canada. A.G. is a fellow of the UCLA medical scientist training program. O.N.W. is an Investigator of the Howard Hughes Medical Institute. Supported by the Physician Scientist Award CA 01551 from the National Cancer Institute (C.L.S.) and by grant CA 53867 from the National Institutes of Health (O.N.W.).

30 December 1993; accepted 9 March 1994

A Dual Embryonic Origin for Vertebrate Mechanoreceptors

Andres Collazo, Scott E. Fraser, Paula M. Mabee*

Neuromasts, the mechanoreceptors of the lateral line system of fishes and aquatic amphibians, have previously been thought to develop exclusively from embryonic epidermal placodes. Use of fate mapping techniques shows that neuromasts of the head and body of zebrafish, Siamese fighting fish, and *Xenopus* are also derived from neural crest. Neural crest migrates away from the neural tube in developing vertebrates to form much of the peripheral nervous system, pigment cells, and skeletal elements of the head. The data presented here demonstrate that neuromasts are derived from both neural crest and epidermal placodes.

Neuromasts are sensory structures of fishes and aquatic amphibians that function to detect vibrations in the nearby water, and thereby facilitate schooling, prey capture, and predator avoidance (*1*). They are predominantly arranged in lines on the body surface and head, and together comprise the lateral line system. Neuromasts display a highly conserved structure, with a core of sensory hair cells that are surrounded and underlain by support cells and are covered with a gelatinous cupula (*1*, *2*). Neuromasts evolved in the common ancestor of vertebrates and are retained in lampreys, sharks and rays, fishes, and aquatic amphibians (Fig. 1). Vertebrates have hair cells in the inner ear that are considered homologous to the hair cells of neuromasts by virtue of their similarity in structure and function.

In amphibians, a variety of classical experimental techniques (*3*–*7*) have demonstrated that neuromasts of the head and body develop from epidermal placodes that all originate on the head. Placodes caudal to the otic capsule migrate from head to tail tip, dropping off clusters of cells that differentiate as neuromasts. Although it is assumed that neuromasts develop in the same manner in teleosts and although postotic placode migration has been documented

A. Collazo and S. E. Fraser, Division of Biology, Beckman Institute 139-74, California Institute of Technology, Pasadena, CA 91125, USA.
P. M. Mabee, Department of Biology, San Diego State University, San Diego, CA 92182–0057, USA.

*To whom correspondence should be addressed.

(8), the data regarding the origin of cranial neuromasts have remained inconsistent. Placodes have been observed in a few species (9, 10), but in other fishes neuromasts appear to erupt without an obvious placodal precursor (11, 12). The observed proximity of neural crest and placodes might be taken to suggest that the neural crest induces placode formation or induces neuromast formation from placodes (13–15).

To define more precisely the origin of lateral line neuromasts, we used vital fluorescent dyes, as recently used to characterize the amphibian trunk neural crest (16). Either neural crest or placode cells were labeled with the lipophilic dye, DiI, and individual embryos were traced and imaged at daily or weekly intervals for up to a month (17). After portions of the neural crest were labeled in cranial and trunk areas (Fig. 2), some embryos were observed with time-lapse photography at intervals of 2 min over a period of 8 hours. Although the overall pathways of neural crest migration were predictable, movements of individual cells were often tortuous and resulted in a marked dispersion from the injection site across much of the cranium or trunk. These observations allowed us to determine that labeled neural crest cells do not transfer dye from labeled to unlabeled cells.

Both the neural crest and epidermal placodes contributed to neuromasts in the teleost fishes *Brachydanio rerio* (Ostariophysi) and *Betta splendens* (Percomorpha) (18) and in an anuran amphibian, *Xenopus laevis*. Cranial neural crest cells (Fig. 2A) contributed to cranial neuromasts in both fishes (Fig. 3, A to D) and to cranial and trunk neuromasts in *Xenopus* (Fig. 4, A to D). DiI-labeled cranial neural crest cells of one *Betta* individual, for example, migrated from a location dorsal to the presumptive lateral line primordia (9) (Fig. 4A). These cells differentiated by 23 days into opercular neuromasts (Fig. 3, B to D), as well as into pigment cells (Fig. 3D) and other neural crest derivatives. Labeled neuromasts were interspersed with unlabeled neuromasts (Fig. 3, C and D). In *Xenopus*, labeled neural crest cells migrated into neural crest derivatives such as branchial arches, passing under regions that form prospective lateral line placodes. Labeled cells were visible in neuromasts of stage 48 *Xenopus* (Fig. 4, B and C) and in the fishes at approximately 3 weeks of age. Neuromasts were identified in vivo by morphology and position, the latter determined by labeling of uninjected controls with the vital dyes 4-Di-2-ASP or methylene blue, which specifically label neuromast hair cells (Fig. 2, D and E). Photoconversion of DiI-labeled neuromasts (19), which were histologically sectioned, confirmed observations in whole animals that both sensory hair cells and peripheral cells of cranial neuromasts were labeled (Fig. 4D), although not all cells of a single neuromast were necessarily labeled.

To determine whether trunk neural crest cells contribute to neuromasts, we injected embryos in the mid to posterior trunk (Fig. 2B), a region caudal to all developing placodes. Similar to results from cranial injections, trunk neural crest cells contribute to neuromasts. The rostrocaudal extent of the injection sites was typically the size of one somite (Fig. 3E). In one fish embryo, the labeled neural crest cells had dispersed as far as 20 somites by 2 days (Fig. 3F). After 23 days, three labeled neuromasts were visible at the same axial levels at which labeled spinal ganglia were present at 2 days (Fig. 3, G and H). In another embryo, two labeled neuromasts were observed at a more posterior site (Fig. 3, I and J). As in the cranial neuromasts, hair cells and peripheral cells were labeled (Fig. 3, H to J).

The same methods allowed us to observe the placodes that contribute to the head lateral lines of teleosts. Cranial placodes were discovered that contribute to the formation of both cranial and trunk neuromasts (Figs. 2C and 4E). We labeled only superficial placodal cells (Fig. 4E), and not the underlying neural crest, which would have given rise to ganglia, pigment cells, and skeletal derivatives (20). Postotic placodes contributed to neuromasts along the dorsal, middle, and ventral trunk lines (Fig. 4F). Teleost neuromasts derived from placodes appeared to differentiate earlier than do neuromasts from neural crest cells. In juvenile *Brachydanio* only two trunk lines are described (8); the middle trunk line that we describe disperses to become less recognizable by the juvenile stage. Cells of the postotic placode also formed a path between neuromasts, and these may be glial cells that wrap the lateral line nerve (21). Although glial cells are thought to arise

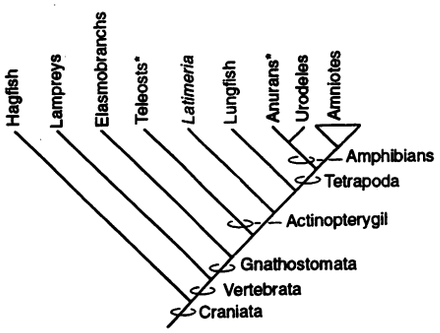

Fig. 1. Phylogeny of living craniates. Neural crest, epidermal placodes, and neuromasts evolved in the common ancestor of vertebrates and are retained in all descendants except amniotes (26, 27). Hair cells are retained in the inner ear of amniotes. The asterisk indicates those taxa from which we found neuromasts to be derived from both placodes and neural crest.

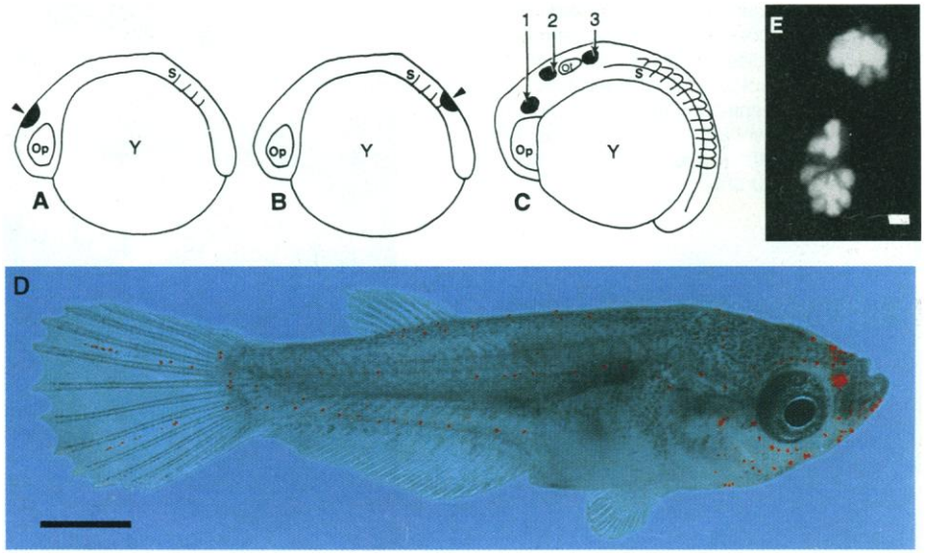

Fig. 2. Injections of teleost embryos (17) and neuromast labeling with 4-Di-2-ASP in fish and amphibians. *Brachydanio* development is described in (28) and *Betta* staging is similar (29). (**A**) Injections into the cranial neural keel (arrowhead); five somites and optic vesicles were present. (**B**) Injections into the trunk neural keel (arrowhead); *Betta*, $n = 3$, and *Brachydanio*, $n = 4$; same stage. (**C**) Superficial placode injections in regions 1 (postoptic), 2 (preotic), and 3 (postotic); *Brachydanio*, $n = 84$; 15 somites, otic vesicle present. Op, optic vesicle; Ot, otic placode; S, somites; Y, yolk. (**D**) Juvenile *Betta* with 4-Di-2-ASP–labeled hair cells in all functional neuromasts of the lateral line system. Each red dot represents from 2 to 16 hair cells. The receptor cells of the nose also label with the dye. Scale bar, 1 mm. (**E**) 4-Di-2-ASP–labeled hair cells in two neuromasts of a stage 50 (30) *Xenopus* tadpole, fluorescent image. Ten hair cells labeled with 4-Di-2-ASP are visible in the lower neuromast. Scale bar, 10 μm.

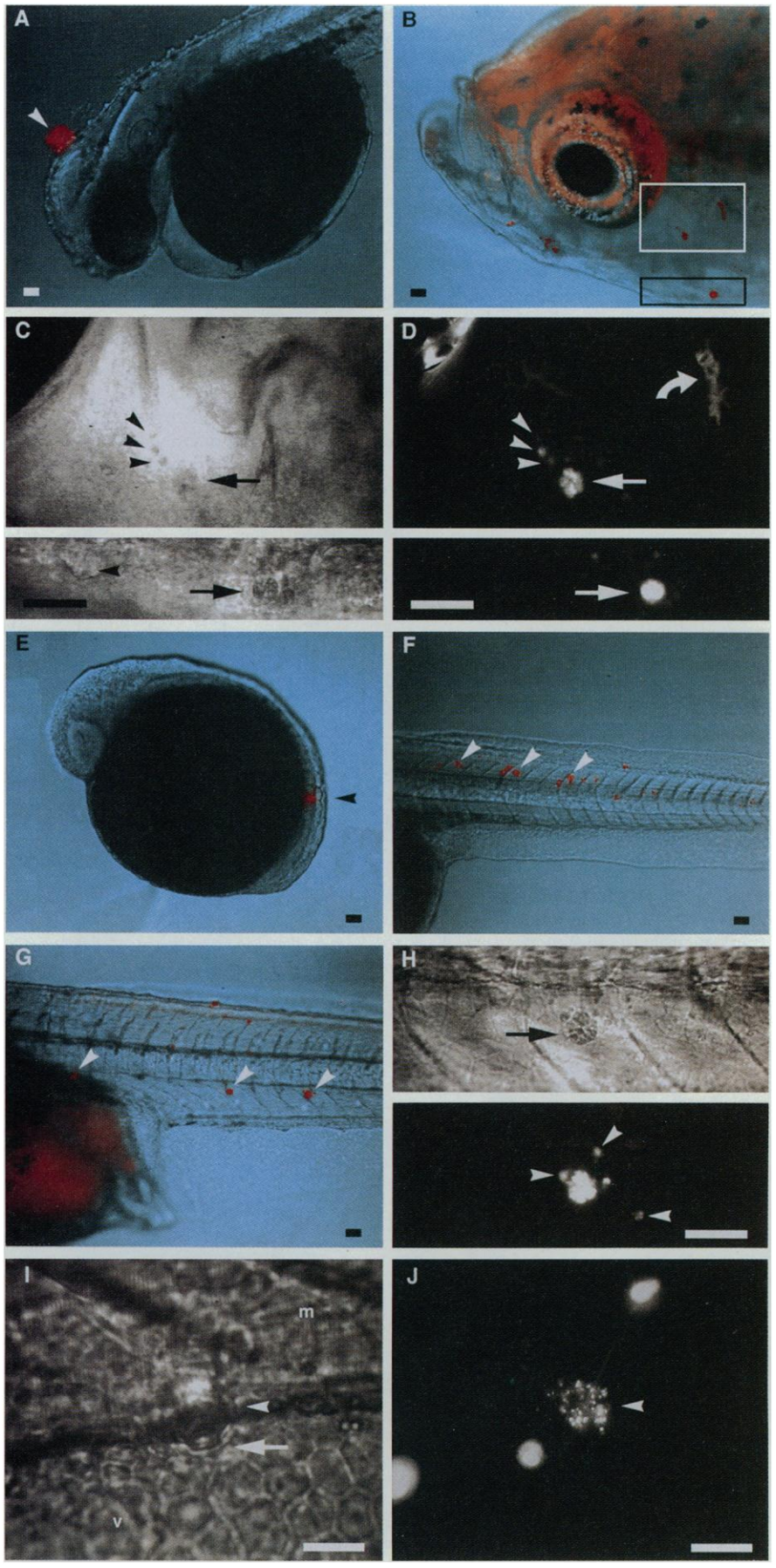

Fig. 3. Labeled neuromasts derived from DiI-labeled neural crest in living *Betta*. Color images are the result of combining bright-field and fluorescent images by computer (*17*). (A to D) *Betta* embryo labeled in the dorsal cranial neural keel. (**A**) Label (arrowhead) is restricted to the dorsal-medial region of the head. The nearest presumptive placode (*9*) is about 175 μm away. At this stage [approximately primordium 22 (*28*)] the posterior trunk primordium is migrating. (**B**) Labeled neuromasts in the ventral opercular region at 23 days. The two boxes enclose labeled neural crest derivatives. The white-boxed region is shown in the top panel of (C) and (D), the black-boxed region in the bottom panel. The red in the eye and dorsal half of the head is due to autofluorescence from iridophores. (**C**) Differential interference contrast (DIC) images of three neuromasts. (Top) A neuromast (arrow) and, dorsorostrally, peripheral cells (arrowheads). (Bottom) Two neuromasts, the right one labeled with DiI (arrow), the left one unlabeled (arrowhead). (**D**) Fluorescent images of the same area shown in (C). (Top) In addition to the labeled neuromasts (arrow) and peripheral cells (arrowheads), there is a labeled pigment cell (curved arrow), an expected neural crest derivative. (Bottom) The right neuromast is labeled with DiI (arrow). (E to H) A *Betta* embryo at three stages after labeling of the trunk neural keel. (**E**) The region initially labeled (arrowhead) is restricted to the posterior trunk of the 14-somite embryo and is about 800 μm from the nearest placode. (**F**) Labeled neural crest has migrated and dispersed across approximately 20 myomeres at primordium stage 22. Note prospective spinal ganglia (arrowheads) at three different segments. (**G**) Three labeled neuromasts (arrowheads) in the ventral line at 23 days. (**H**) DIC image (top) and fluorescent image (bottom) of the posterior-most labeled neuromast in (G). (Bottom) Note the labeled cells (arrowheads) peripheral to the neuromast (arrow). (**I**) DIC image of a posterior neuromast (arrowhead) in ventral line of a different *Betta* embryo at 21 days. Arrow points to apical end. Abbreviations: m, muscle cells and v, ventral fin. (**J**) Fluorescent image of neuromast (arrowhead) in (I), neuromast label resulting from midtrunk neural crest injection. Scale bars represent 50 μm.

from the neural crest (*20, 22*), our data support a placodal origin in some cases, as described in amphibians (*5*) and demonstrated in studies on the olfactory placode in birds and mammals (*23*).

A neural crest origin for neuromasts is consistent with the observation that neural crest cells migrate to positions close to the neuromasts in teleosts (*13*). The labeled neuromasts that we observed may result from neural crest cells that differentiate directly into neuromasts or that disperse first into the placode or migrating primordium. A dual embryonic origin for a peripheral nervous system structure should not be surprising because, for example, both neural crest and placodes are known to contribute to cranial ganglia (*20, 22, 24*). Neural crest and lateral line placodes may be able to compensate for each other in the formation of neuromasts, as they appear to do in the formation of cranial ganglia (*24*). A neural crest origin also explains the normal development of neuromasts after primordium removal in fishes (*25*) and amphibians (*7*). Moreover, our results raise the question of whether hair cells of the inner ear may similarly originate from both neural crest and the otic placode.

Many of the novel structures that evolved in vertebrates and distinguish them from their ancestors are embryonically derived from neural crest or various epidermal placodes (*15, 22, 26*). Our data raise the possibility that a dual neural crest and epidermal origin of neuromasts may have evolved in the common ancestor of vertebrates.

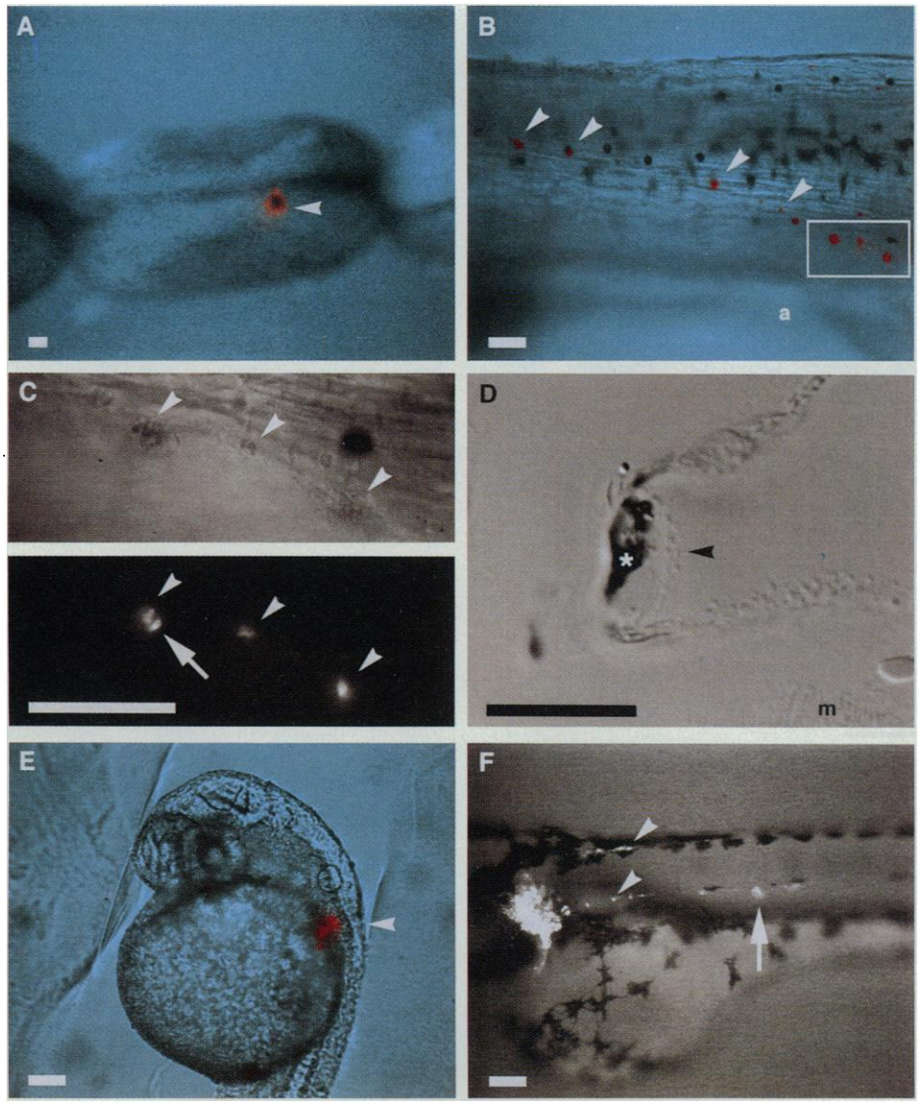

Fig. 4. Labeled neuromasts derived from DiI-labeled neural crest in living *Xenopus* and from DiI-labeled placodes in *Brachydanio*. (A to C) A *Xenopus* embryo labeled in the cranial neural crest at stage 15 (*30*) shown at two later stages. Lateral view, anterior to right. (**A**) Label is restricted to the dorsal portion of the neural tube at stage 17 (arrowhead) and is separated from the presumptive placodes (*21*) by 200 μm. (**B**) Labeled neuromasts in the trunk line (arrowheads) at stage 48. Three neuromasts enclosed by the white box are shown at higher magnification in (C). Abbreviation: a, anus. (**C**) DIC image (top) over the fluorescent image (bottom) of three labeled neuromasts (arrowheads) in the region enclosed by the white box in (B). Note the hair cell morphology of labeled cells (arrow). (**D**) DIC image of photoconverted DiI in a *Xenopus* neuromast (10-μm-thick plastic section). Asterisk denotes label inside neuromast. Arrowhead points to apical end of neuromast. Abbreviation: m, muscle cells. (E to F) Labeling of the postotic placode of *Brachydanio* reveals the placodal origin of trunk neuromasts and, possibly, of glia wrapping the posterior lateral line nerves. Three posterior lateral lines arise from the postotic placode (n = 6). Embryos were labeled superficially before posterior placode cells began to migrate (*8, 28*). (**E**) DiI-labeled postotic placode (arrowhead) at the 26-somite stage. (**F**) Same embryo 2 days later. Dorsal and main trunk lines are distinct (arrowheads) in this fluorescent image. Ventral line primordium migrates from main trunk line (arrow) ventrally and then runs parallel to main trunk line. Scale bars represent 100 μm, except for (D), where the scale bar represents 20 μm.

REFERENCES AND NOTES

1. J. Atema, R. R. Fay, A. N. Popper, W. N. Tavolga, Eds., *Sensory Biology of Aquatic Animals* (Springer-Verlag, New York, 1988).
2. J. E. Jones and J. T. Corwin, *J. Neurosci.* **13**, 1022 (1993).
3. R. G. Harrison, *Arch. Mikrosk. Anat. Entomol.* **63**, 35 (1904).
4. L. S. Stone, *J. Exp. Zool.* **35**, 421 (1922); *Anat. Rec.* **48**, 64 (1931); *J. Comp. Neurol.* **68**, 83 (1937).
5. _____, *J. Comp. Neurol.* **57**, 507 (1933).
6. R. Winklbauer, *Prog. Neurobiol.* **32**, 181 (1989).
7. R. Winklbauer and P. Hausen, *J. Embryol. Exp. Morphol.* **88**, 193 (1985).
8. W. K. Metcalfe, *J. Comp. Neurol.* **238**, 218 (1985); _____, C. B. Kimmel, E. Schabtach, *ibid.* **233**, 377 (1985).
9. H. Wilson and J. Mattocks, *Anat. Anz.* **13** (1897), H. Wilson, *Bull. U.S. Fish. Comm.* **9**, 209 (1891); B. Lekander, *Acta Zool.* **30**, 1 (1949).
10. R. G. Northcutt, in *The Evolutionary Biology of Hearing*, D. Webster, R. Fay, A. Popper, Eds. (Springer-Verlag, New York, 1992), pp. 21–47.
11. F. L. Landacre, *J. Comp. Neurol.* **20**, 309 (1910).
12. _____ and A. C. Conger, *ibid.* **23**, 576 (1913); H. Vischer, *Brain Behav. Evol.* **33**, 205 (1989).
13. C. H. J. Lamers, J. W. H. M. Rombout, L. P. M. Timmermans, *J. Embryol. Exp. Morphol.* **62**, 309 (1981).
14. J. Holtfreter, *Wilhelm Roux Arch. Entwicklungsmech. Org.* **127**, 619 (1933).
15. D. M. Noden, in *Developmental and Evolutionary Aspects of the Neural Crest*, P. Maderson, Ed. (Wiley, New York, 1987), pp. 89–119; *Development* **103**, 121 (1988); *Brain Behav. Evol.* **38**, 190 (1991).
16. A. Collazo, M. Bronner-Fraser, S. E. Fraser, *Development* **118**, 363 (1993).
17. A 0.5% solution of 1,1-dioctadecyl-3,3,3′,3′-tetramethylindocarbocyanine perchlorate (DiI; Molecular Probes, Eugene, OR) was made up in 100% ethanol, and the dye was injected at this concentration or diluted for some *Xenopus* (*16*). Quartz micropipettes of approximately 20-μm tips were back-filled with DiI solution and attached to a Picospritzer (General Valve, Fairfield, NJ). Teleost embryos were dechorionated and held for injection in 3% methyl cellulose as described (*28*). DiI was injected into neural folds, tube, or keel, which contain presumptive neural crest cells. Living embryos were anesthetized (0.2% methanesulfonate) and placed in petri dishes containing shal-

low depressions in 2% agar. Labeled cells were visualized on a Zeiss epifluorescence microscope with objectives ranging from ×2.5 to 40 at an excitation wavelength of 540 to 560 nm. Data were recorded onto a video optical disk recorder (OMDR) with a light-intensifying camera (Hamamatsu SIT) and image processor (Imaging Technology 151, Woburn, MA) and the VidIm software package (G. R. Belford, J. Stollberg, S. E. Fraser, unpublished data) (*16*).
18. *Betta splendens* (Siamese fighting fish) larvae appear to be hardier than *Brachydanio rerio*, with greater tolerance to repeated anesthesia and a higher rate of survival to the age of 4 weeks.
19. J. C. Izpisúa-Belmonte, E. M. De Robertis, K. G. Storey, C. D. Stern, *Cell* **74**, 645 (1993).
20. N. M. Le Douarin, *The Neural Crest* (Cambridge Univ. Press, Cambridge, 1982).
21. A. Collazo, P. M. Mabee, S. E. Fraser, data not shown.
22. B. K. Hall and S. Horstadius, *The Neural Crest* (Oxford Univ. Press, New York, 1988).
23. G. F. Couly and N. M. Le Douarin, *Dev. Biol.* 110, 422 (1985); M. I. Chuah and C. Au, *J. Neurosci. Res.* **29**, 172 (1991).
24. M. L. Kirby, *Cell Tissue Res.* **252**, 17 (1988); *J. Neurosci.* **8**, 1089 (1988).
25. S. W. Bailey, *J. Exp. Zool.* **76**, 187 (1937).
26. R. G. Northcutt and C. Gans, *Q. Rev. Biol.* **58**, 1 (1983).
27. P. Forey and P. Janvier, *Nature* **361**, 129 (1993).
28. M. Westerfield, Ed., *The Zebrafish Book* (Univ. of Oregon Press, Eugene, OR, 1993).
29. P. M. Mabee, unpublished data.
30. P. D. Nieuwkoop and J. Faber, *Normal Table of Xenopus laevis (Daudin)* (North-Holland, Amsterdam, Netherlands, 1967).
31. We thank R. G. Northcutt, M. Bronner-Fraser, S. Cohen-Cory, C. Gans, J. Shih, G. N. Serbedzija, and S. C. Smith for comments. Supported in part by NSF grant 8821241 and AAFD and RSCA grants from San Diego State University (to P.M.M.), USPHS grants HD25138 (to M. Bronner-Fraser) and HD26864 (to S.E.F.), and a fellowship from the Muscular Dystrophy Association (to A.C.).

21 June 1993; accepted 3 March 1994

Association of Intestinal Peptide Transport with a Protein Related to the Cadherin Superfamily

Anne H. Dantzig,* JoAnn Hoskins, Linda B. Tabas, Stuart Bright, Robert L. Shepard, Ivan L. Jenkins, Dale C. Duckworth, J. Richard Sportsman, Daniel Mackensen, Paul R. Rosteck Jr., Paul L. Skatrud*

The first step in oral absorption of many medically important peptide-based drugs is mediated by an intestinal proton-dependent peptide transporter. This transporter facilitates the oral absorption of β-lactam antibiotics and angiotensin-converting enzyme inhibitors from the intestine into enterocytes lining the luminal wall. A monoclonal antibody that blocked uptake of cephalexin was used to identify and clone a gene that encodes an approximately 92-kilodalton membrane protein that was associated with the acquisition of peptide transport activity by transport-deficient cells. The amino acid sequence deduced from the complementary DNA sequence of the cloned gene indicated that this transport-associated protein shares several conserved structural elements with the cadherin superfamily of calcium-dependent, cell-cell adhesion proteins.

Several peptidyl mimetic drugs, such as β-lactam antibiotics and angiotensin-converting enzyme inhibitors, are readily absorbed orally in humans. These drugs along with di- and tripeptides share a transport mechanism that is a major route for the assimilation of peptide nutrients in the intestine (*1*). Substrates are cotransported with protons and concentrated initially within the intestinal enterocyte before exiting the serosal side of the enterocyte (*2*). Information about the transporter would be helpful in the rational design of new oral small peptidyl-like therapeutic drugs.

When confluent, the human colon adenocarcinoma Caco-2 cells differentiate and acquire intestinal enterocytic-like properties (*3*). These cells possess a proton-dependent peptide transporter that takes up β-lactams including cephalexin, cefaclor, and loracarbef (*4*). Properties of this transporter closely resemble those of the intestinal peptide transporter of other species (*4*). The biochemical purification of the rabbit intestinal peptide transporter revealed a ~127-kD integral membrane glycoprotein that exhibits transport activity when reconstituted into liposomes (*5*). The gene encoding this transporter, however, has not been identified.

To identify the human intestinal peptide transporter, monoclonal antibodies were prepared that blocked cephalexin uptake into Caco-2 cells (*6*), and monoclonal antibody (mAb) 13G6 was selected. Membrane proteins of Caco-2 cells were separated by SDS–polyacrylamide gel electrophoresis (PAGE) and immunoblotted with antibody (Fig. 1, lane 1). A single protein band with an apparent mass of 120 ± 10 kD was detected in Caco-2 membranes. Deglycosylation with endoglycosidase F before SDS-PAGE shifted the immunoreactive band to ~100 kD (*7*). A survey of membranes from several human cell lines indicated the presence of the 120 ± 10 kD protein in cells derived from the gastrointestinal (GI) tract but not in cell lines derived from other tissues (Fig. 1). Immunohistochemical staining of normal human tissues indicated the presence of antigen in tissues along the GI tract (jejunum, duodenum, ileum, and colon) and the pancreatic ducts and the absence of antigen on specimens examined from the kidney, lung, liver, brain, adrenal gland, and skin (Fig. 2).

A Caco-2 complementary DNA (cDNA) library constructed in λgt11 (*8*) was screened with mAb 13G6 for expression of the antigen. A ~750–base pair (bp) cDNA fragment was repeatedly recovered. The deduced amino acid sequence of the open reading frame (ORF) of this cDNA showed a protein with mass of ~35 kD, considerably smaller than the expected size of ~100 kD. Therefore, a new cDNA

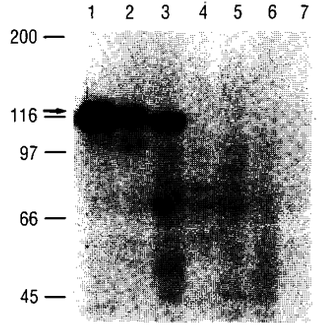

Fig. 1. Immunoblot analysis of membranes from human cell lines with mAb 13G6 to transporter. Membrane proteins (~100 μg per lane) were separated by 8% SDS-PAGE for ~14 hours (*21*). Gel was electroblotted onto nitrocellulose paper; blocked with 3% bovine serum albumin and 0.1% Triton X-100, 150 mM NaCl, 1 mM EDTA, 0.01 M tris-HCl (pH 7.5); and reacted with purified mouse antibody to transporter (20 μg/ml) followed by incubation with goat antibody to mouse [^{125}I]immunoglobulin G (IgG) (0.3 μCi/ml). Lane 1, colon Caco-2; lane 2, colon HT-29; lane 3, colon COLO 320; lane 4, lymphoblast CCRF-CEM; lane 5, lymphoblast IM-9; lane 6, neuroblastoma SK-N-MC; lane 7, glioblastoma U-373. The arrow indicates the band for a 120 ± 10 kD protein, the putative transporter. Molecular masses are given to the left in kilodaltons.

A. H. Dantzig, J. Hoskins, L. B. Tabas, S. Bright, R. L. Shepard, I. L. Jenkins, D. C. Duckworth, P. R. Rosteck Jr., P. L. Skatrud, Lilly Research Laboratories, Eli Lilly and Company, Indianapolis, IN 46285, USA.
J. R. Sportsman, Terrapin Technologies, San Francisco, CA 94080, USA.
D. Mackensen, Hybritech Inc., San Diego, CA 92121, USA.

*To whom correspondence should be addressed.